Coherent anti-Stokes Raman scattering spectral interferometry: determination of the real and imaginary components of nonlinear susceptibility $\chi^{(3)}$ for vibrational microscopy

Conor L. Evans, Eric O. Potma, and X. Sunney Xie

Department of Chemistry and Chemical Biology, Harvard University, 12 Oxford Street, Cambridge, Massachusetts 02138

Received June 10, 2004

We demonstrate coherent anti-Stokes Raman scattering (CARS) heterodyne spectral interferometry for retrieval of the real and imaginary components of the third-order nonlinear susceptibility ($\chi^{(3)}$) of molecular vibrations. Extraction of the imaginary component of $\chi^{(3)}$ allows a straightforward reconstruction of the vibrationally resonant signal that is completely free of the electronic nonresonant background and resembles the spontaneous Raman spectrum. Heterodyne detection offers potential for signal amplification and enhanced sensitivity for CARS microscopy.

OCIS codes: 110.0180, 180.3170, 300.6230.

Since its revival in 1999, coherent anti-Stokes Raman scattering (CARS) microscopy has proved to be a powerful method for sensitive vibrational imaging of biological samples.[1] The vibrational contrast in CARS imaging results from the Raman activity of endogenous molecules, which circumvents the need for fluorescent labels. CARS microscopy has been successfully applied to live cell imaging[1] and intracellular organelle tracking[2] and holds great promise for noninvasive tissue imaging. However, the sensitivity of CARS microscopy is limited by a nonresonant background that is independent of the Raman shift. CARS arises from the third-order nonlinear susceptibility $\chi^{(3)}$, which is the sum of a vibrationally resonant part $\chi^{(3)}_{\mathrm{res}}$ and a nonresonant electronic contribution $\chi^{(3)}_{\mathrm{nr}}$. The latter generates a nonresonant field that not only introduces an offset that can be overwhelming at times but also distorts the resonant spectral profile through interference with the resonant field. This makes it difficult to assign CARS spectra based on the wealth of spectral assignments in the Raman literature. Polarization-sensitive detection[3] and time-resolved CARS[4] have been developed to suppress the nonresonant background but are always accompanied by signal attenuation. To improve the sensitivity and spectral selectivity of CARS microscopy, an approach is needed that suppresses the nonresonant background while allowing complete extraction of the resonant vibrational information.

One solution to this problem lies in taking advantage of a fundamental difference between the resonant and the nonresonant nonlinear susceptibilities: Whereas $\chi^{(3)}_{\mathrm{nr}}$ has only a real component, $\chi^{(3)}_{\mathrm{res}}$ has both real and imaginary parts. It was well established that the spectrum of the imaginary part of $\chi^{(3)}_{\mathrm{res}}$, $\mathrm{Im}(\chi^{(3)}_{\mathrm{res}})$, is proportional to the spontaneous Raman spectrum.[5] Isolating the imaginary component thus gives only resonant information, free of the nonresonant background. Conventional CARS techniques measure $|\chi^{(3)}|^2$, which entangles the real and imaginary components. A direct means of extracting the imaginary part is heterodyne mixing with a local oscillator field. Heterodyne detection offers a number of attractive qualities. First, it allows a direct comparison with Raman spectral profiles without the complication of a nonresonant background. Second, the heterodyne signal is linearly proportional to the concentration, which permits a straightforward quantitative interpretation of images. Last, heterodyne mixing provides the possibility of interferometric CARS signal enhancement by mixing with a strong local oscillator field.

The potential of CARS interferometry was previously demonstrated by suppressing the nonresonant background in the gas phase with narrowband laser excitation.[6] In this Letter we resolve the real and imaginary parts of $\chi^{(3)}$ of vibrational bands in the condensed phase with broadband CARS spectral interferometry. Although this information is in principle accessible through time-domain CARS interferometry,[7] extracting accurate phase information from time-resolved traces is difficult in practice. Spectral interferometry has many advantages over temporal interferometry, including better signal-to-noise characteristics[8] and insensitivity to temporal pulse jitter. In addition, acquisition times can be much shorter because spectral interferometry requires no scanning and the amplitude and phase can be extracted through simple trigonometry.

In our spectral interferometry method, a broadband CARS field $E_s(\omega)$ from the sample arm interferes with a broadband CARS local oscillator field E_{lo} generated from a nonresonant sample in the local oscillator arm. The interference appears as a sinusoidal modulation on the detected spectral intensity:

$$S_{\mathrm{CARS}}(\omega) = |E_{\mathrm{lo}}|^2 + |E_s(\omega)|^2 + 2|E_{\mathrm{lo}}E_s(\omega)|\cos\,\Phi(\omega)\,, \tag{1}$$

where $\Phi(\omega) = \omega\tau + \phi_s(\omega) + \phi_{\mathrm{inst}}(\omega)$ is the total phase difference between the arms. Here τ is the temporal delay between the two arms of the interferometer,

0146-9592/04/242923-03$15.00/0

$\phi_s(\omega)$ is the phase difference introduced by the sample, and $\phi_{\text{inst}}(\omega)$ is the relative phase delay due to optical components in the interferometer. The phase information is encoded in the spectral fringe spacing and can be extracted from the spectral interferogram.[9] Once $\phi_s(\omega)$ is known, the real and imaginary components of $\chi^{(3)}(\omega)$ can be readily determined.

The experimental setup (Fig. 1) is based on two synchronized mode-locked Ti:sapphire lasers and follows an excitation scheme similar to that in multiplex CARS spectroscopy.[10] For this experiment the Raman shift was tuned to the CH-stretch vibrational region of dodecane, with the picosecond pump laser set at 712.5 nm and the femtosecond Stokes laser centered at 897 nm (FWHM 140 cm^{-1}). In the sample arm of the Mach–Zehnder interferometer, the pump and Stokes beams were focused onto a glass–dodecane interface by use of a high-numerical-aperture lens. An identical lens was used in the local oscillator arm to generate the local oscillator field from a glass coverslip–air interface. Both the CARS signal and the local oscillator fields were collected in the epi direction,[11] separated from the pump and Stokes beams by dichroic mirrors, and combined on a cubic beam splitter. Spectral interferograms were monitored with a spectrometer equipped with a CCD. Typical integration times of 5 s were used with 30 mW of average power for each beam at the sample.

Spectrally resolved phase information was extracted from the interferograms with a method developed by Lepetit *et al.*[9] Briefly, the CARS beam from the sample was passed through a quarter-wave plate and converted into a circular polarized beam. After combination with the local oscillator CARS beam at the cubic beam splitter, a polarizing beam splitter set at 45° to the local oscillator beam polarization split the mixed CARS beam into two orthogonally polarized components. These two linearly polarized beams were then spectrally dispersed, and the two separate interferograms were simultaneously detected by the CCD. After the homodyne terms were independently determined, the heterodyne parts were isolated. Because there is a $\pi/2$ phase shift between the two heterodyne contributions, dividing one by the other yields the tangent of total spectral phase $\Phi(\omega)$.

To isolate $\phi_s(\omega)$ from the total phase of the sample, a reference measurement is needed that provides the spectral reference phase $\Phi_{\text{ref}}(\omega) = \omega\tau + \phi_{\text{inst}}(\omega)$. Since $\phi_s(\omega)$ arises only from a resonance, a nonresonant reference sample should be used. As we examined dodecane in the CH-stretch vibrational region, we used fully deuterated dodecane as the reference sample to ensure that the material properties remained nearly identical between the two measurements. A flow cell was used to keep the delay between the two arms identical when switching between the resonant and reference samples. Subtraction of $\Phi_{\text{ref}}(\omega)$ from $\Phi(\omega)$ yields $\phi_s(\omega)$. The path length difference between the arms was found to be stable during the collection time window.

Figure 2 shows two spectral interferograms obtained from both polarization components that were collected from a nonresonant sample. The fringes are the result of a 1-ps path-length difference between the arms. This offset results in the linear spectral phase ($\omega\tau$) that spans the spectral window. The recording of this spectral interferogram required no scanning, was shot noise limited, and was completely insensitive to temporal laser fluctuations.

When the nonresonant sample is replaced by a resonant sample, it is straightforward to ascertain the resonant spectral phase profile. Figure 3(a) shows the amplitude and phase of the dodecane CH-stretch region. The phase shows several maxima. If there was a single spectral resonance, a single phase swing from zero to π centered on that peak would be expected. In this case, however, there is a cluster of spectral resonances that interfere with one another, giving rise to the complex phase profile.

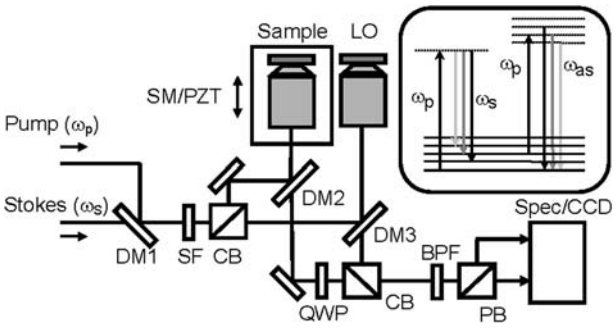

Fig. 1. Schematic of the CARS spectral interferometer. The interferometer consists of a sample arm and a local oscillator (LO) arm. The length of the sample arm is adjustable for phase delay control. DM1, long-wave-pass dichroic mirror for combining pump and Stokes beams; DM2, DM3, shortwave-pass dichroic mirrors; SF, spectral filter (Schott RG695); CB, cubic 50% beam splitter; SM, stepper motor; PZT, piezoelectric transducer; QWP, quarter-wave plate; BPF, bandpass filter (600 nm, 40-nm bandwidth); PB, polarizing beam splitter; Spec, grating spectrometer; CCD, liquid-nitrogen-cooled charge-coupled device. Two identical oil immersion lenses are used (Nikon Plan Apo, 60×, N.A. of 1.4). Inset, CARS energy diagram for picosecond pump and femtosecond Stokes beams.

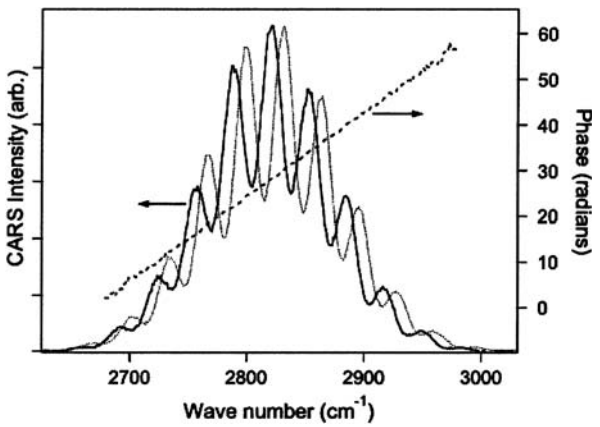

Fig. 2. CARS spectral interferograms of two simultaneously collected orthogonal polarizations from a nonresonant sample (glass coverslip) with the arms offset by 1 ps (solid and dotted curves). The extracted $\Phi_{\text{ref}}(\omega)$ is indicated by the dashed curve.

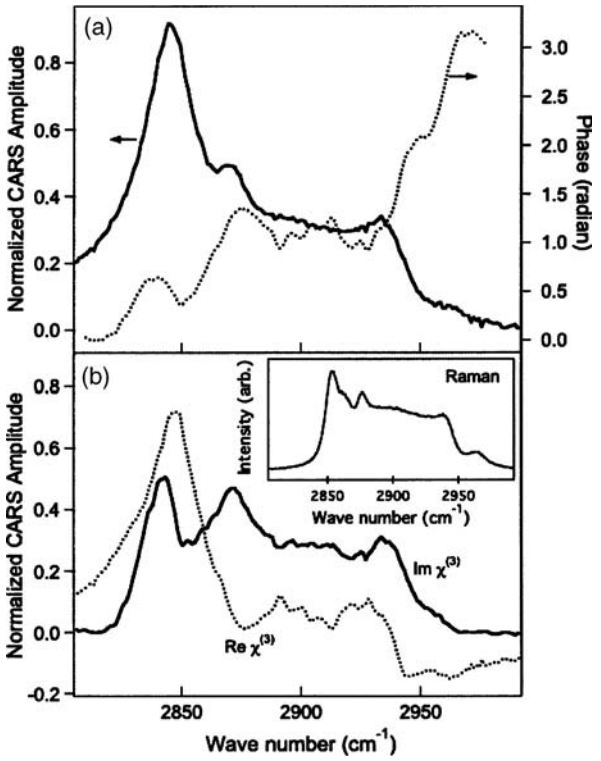

Fig. 3. CARS spectral amplitude and phase of the CH-stretching vibrational band of dodecane. (a) Extracted CARS amplitude (solid curve) and phase (dotted curve) from the spectral interferograms. The CARS spectrum was normalized by the nonresonant CARS spectrum of the local oscillator arm. (b) Reconstructed real $\{|E_s(\omega)|\cos[\phi_s(\omega)] - |E_{nr}(\omega)|$, dotted curve$\}$ and imaginary $\{|E_s(\omega)|\sin[\phi_s(\omega)]$, solid curve$\}$ parts of the CARS spectrum. Inset, Raman spectrum of dodecane in the CH-stretch vibrational range. The spectrum was measured with a Raman microspectrometer with a 1-min integration time.

The real and imaginary components of $\chi^{(3)}$ can readily be calculated from the amplitude and phase [Fig. 3(b)]. The imaginary $\chi^{(3)}$ spectrum is in good agreement with the corresponding Raman spectrum, shown in the inset of Fig. 3(b). The reconstructed spectrum is purely resonant and free of nonresonant background contributions, with all the features of the Raman spectrum reproduced.[12] This demonstrates that heterodyne CARS spectral interferometry provides a means of rapid Raman microspectroscopy, particularly in regions of the vibrational spectrum, such as the fingerprint region, that are too congested to access with conventional CARS spectroscopy.

In conclusion, we have shown that heterodyne CARS interferometry can be used to extract amplitude and phase information from $\chi^{(3)}$ molecular vibrational resonances, leading to complete suppression of the nonresonant background. Unlike conventional CARS signals that are complicated by mixing with nonresonant components, the imaginary part of $\chi^{(3)}$ can be directly equated to Raman spectra. In addition, since the isolated signal comes from the heterodyne term, it is linear with concentration and lends itself immediately to quantitative analysis. Moreover, signal amplification through heterodyne detection offers promise for further increasing the sensitivity of CARS microscopy. As we have shown, CARS heterodyne interferometry can be readily performed in the epi direction, which offers prospects for high-sensitivity CARS tissue imaging.

We thank Brian English for his technical help with the flow cells. This research was funded by the National Science Foundation and the National Institutes of Health. C. L. Evans acknowledges the National Science Foundation for a Graduate Research Fellowship. X. S. Xie's e-mail address is xie@chemistry.harvard.edu.

References

1. J.-X. Cheng and X. S. Xie, J. Phys. Chem. B **108,** 827 (2004).
2. X. L. Nan, J.-X. Cheng, and X. S. Xie, J. Lipid. Res. **44,** 2202 (2003).
3. J.-X. Cheng, L. D. Book, and X. S. Xie, Opt. Lett. **26,** 1341 (2001).
4. A. Volkmer, L. D. Book, and X. S. Xie, Appl. Phys. Lett. **80,** 1505 (2002).
5. R. W. Hellwarth, Prog. Quantum Electron. **5,** 1 (1977).
6. Y. Yacoby and R. Fitzgibbon, J. Appl. Phys. **51,** 3072 (1980).
7. C. Vinegoni, J. S. Bredfeldt, D. L. Marks, and S. A. Boppart, Opt. Express **12,** 331 (2004), http://www.opticsexpress.org.
8. J. F. de Boer, B. Cense, H. Park, M. C. Pierce, G. J. Tearney, and B. E. Bouma, Opt. Lett. **28,** 2067 (2003).
9. L. Lepetit, G. Cheriaux, and M. Joffre, J. Opt. Soc. Am. B **12,** 2467 (1995).
10. J.-X. Cheng, A. Volkmer, L. D. Book, and X. S. Xie, J. Phys. Chem. B **106,** 8493 (2002).
11. A. Volkmer, J.-X. Cheng, and X. S. Xie, Phys. Rev. Lett. **87,** 023901 (2001).
12. The subtle differences between the Raman and the Im$[\chi^{(3)}]$ spectra might be attributed to Raman depolarization effects.